Full title: Electron microscopic analysis of the exo-skeleton of hadal zone amphipod *Hirondellea gigas*

Short title: The inorganic components of the hadal zone amphipod

Authors: Hideki Kobayashi[1)], Hirokazu Shimoshige[2)], Yoshikata Nakajima[2)], Wataru Arai[1)], and Hideto Takami[1)]

1) Japan Agency for Marine-Earth Science and Technology (JAMSTEC) 2-15 Natsushima, Yokosuka, 237-0061, Japan

2) Bio-nano Electronics Research Centre, Toyo University, 2100 Kujirai, Kawagoe, Saitama 350-8585, Japan

Abstract

The amphipod *Hirondellea gigas* inhabits the deepest regions of the oceans in extra high-pressure. However, the mechanisms by which they adapt to their high-pressure environments remain unknown. In this study, we investigated elements of the exoskeleton of *H. gigas* captured from the deepest points of the Mariana Trench. The *H.*

gigas exoskeleton contained aluminum, as well as a major amount of calcium carbonate. Unlike other accumulated metals, aluminum was distributed on the surface of exoskeletons. To investigate how *H. gigas* obtains aluminum, we conducted a metabolome analysis and found that gluconic acid/gluconolactone was capable of extracting metals from the sediment under the habitat conditions of *H. gigas*. The extracted aluminum ions are transformed into the gel state of aluminum hydroxide in alkaline seawater, and this gel covers the body to protect the amphipod. The aluminum gel would be one of good materials to adapt to such high-pressure environment.

Introduction

The deepest bottom of the ocean is an extreme environment characterized by extra-high pressures, low temperatures, and oligotrophy, and few animals can adapt to such extreme environments [1-3]. The amphipod *Hirondellea gigas* is a resident of the deepest points of the Mariana Trench (Challenger Deep), the Philippine Trench, the Izu-Ogasawara Trench, and the Japan Trench, where it inhabits depths greater than 8,000 m [4-8]. It has been reported that *H. gigas* produces a number of polysaccharide

hydrolases as digestive enzymes and survive in oligotrophic environments by obtaining sugars from degradable plant debris using such enzymes [6, 7]. We attempted to capture animals using baited traps along deep-sea points, and these amphipods were the only catch [5-7]. Amphipods are the main prey for deep-sea fish, and the distribution of deep-sea snailfish slightly overlaps with that of *H. gigas* at approximately 8,000 m [9, 10]. The deep-sea snailfish have been found at depths of 8,145 m in the Mariana Trench, which is the deepest record of fishes [11]. The bottom of the deep trench around 10,000 m in depth seems to be advantageous for *Hirondellea* species to escape from their predators. The extra-high pressure in the deep sea affects the various chemical components of organisms. Calcium carbonate is an important component of crustacean exoskeletons; however, it dissolves in seawater deeper than approximately 4,000-5,000 m (Carbonate Compensation Depth, CCD) [12], and actually they cannot migrate in the deep-sea floor below CCD [13, 14]. Recently, a few species in the crustacean and foraminifera were found in the region slightly deeper than CCD [15-17]. Moreover, lots of foraminifera found in bottom of the Challenger Deep were organic-walled allogromiids, which do not have calcareous wall [18]. Because the habitable zone of *H.*

49 *gigas* is at depths greater than 8,000 m, they hardly to use calcium carbonate in their
50 exoskeleton. However, the mechanisms by which they adapt to their high-pressure
51 environments remain unknown.
52 Thus, we investigated elements of the exoskeleton of *H. gigas* specimens captured from
53 the deepest points of the Mariana Trench (Challenger Deep) as well as the
54 Izu-Ogasawara Trench by electron microscopy analyses. We found that aluminum
55 would reinforce calcium carbonate, which is major component of the *H. gigas*
56 exoskeleton.
57

58 # Materials and Methods

59 ## Amphipods

60 The deep-sea amphipod *Hirondellea gigas* was captured from Challenger Deep in the
61 Mariana Trench (depth: 10,898 m) as well as the Izu-Ogasawara Trench (depth: 9,450
62 m) as described in a previous manuscript [6, 7]. *H. gigas* is >3 cm from the head to tail.
63 We also purchased amphipods from Yokoebi-ya (Fukui, Japan). The coastal amphipods
64 were captured from the seashore of the Maizuru Bay in Japan, and their size is <2-3 mm

65 from the head to tail. All *H. gigas* or the coastal amphipods were stored in storage bags
66 at -80°C without any selection. We selected amphipods for all analysis, randomly.

67 Sediment sample

68 We collected sediment samples from Challenger Deep in the Mariana Trench (11
69 22.030°N, 142 26.032°E, depth: 10,897 m) using the unmanned remotely operated
70 underwater vehicle "KAIKO" on May 4, 1996. The sediment sample was stored at
71 -80°C.

72 Electron microscopy observations and EDS analyses

73 Scanning electron microscopy (SEM) and EDS analysis

74 The freeze-dried amphipod sample was set on the stage of a SEM, which was covered
75 with a silicon plate and carbon tape to avoid EDS signals from the stage. The
76 exoskeleton of the amphipod was observed with a scanning electron microscope (SEM)
77 (SU6600, Hitachi High-Technologies Co., Tokyo, Japan) under accelerating voltages of
78 20 kV, which have been previously described, and the elementary components were
79 analyzed by energy-dispersive X-ray spectroscopy (EDS) (X-Max^N, Oxford).

80 Scanning transmission electron microscopy (TEM) and EDS analysis

We removed the exoskeleton from *H. gigas* and washed it with DDW and ethanol to avoid inhibition by the oil component during the electron microscope observations. Pieces of *H. gigas* exoskeleton obtained after a milling treatment were placed on a TEM grid (200 mesh Cu Formvar/carbon-coated grid, JEOL) and observed under a TEM (JEM-2100, JEOL) with an accelerating voltage of 200 kV. A scanning TEM (STEM)-EDS analysis was performed at 200 kV with an accumulation time of 60 s.

Identification of the calcium carbonate using X-ray powder diffraction (XRD) analysis

The exoskeletons of *H. gigas* were removed from individuals with tweezers and dissecting scissors, and washed with methanol and chloroform. After dried the exoskeletons, we cut and crushed them into powder for XRD analysis. The exoskeleton powder was analyzed by X-ray diffractometry (SmartLab, Rigaku), with a Cu radiation source (Kα =1.5418 Å) at 45 kV and 200 mA. The 2θ scan speed, step width, and range was 21.6746 deg/min, 0.02 deg, and 20 to 50 deg. We identified calcium carbonate in the exoskeleton powder through the database (International Centre for Diffraction Data (ICDD)) search of obtained peak positions.

97 **Extraction of metal ions and gluconic acid/gluconolactone from**
98 **amphipod**

99 We carefully removed the exoskeleton from amphipod with tweezers and dissecting
100 scissors. Then, we subdivided the exoskeleton in the 0.1N sodium acetate buffer (pH
101 4.0), and stirred this suspension with a vortex mixer to extract metal ions and
102 gluconolactone/gluconic acid in the exoskeleton. After centrifugation (2,000 x g, 10
103 min, 4°C), the supernatant was collected, and the precipitated exoskeleton was
104 suspended in the same buffer. Then, we repeated stirring and centrifugation of
105 suspension. Both supernatants were collected, and used for the measurement of metal
106 ions or gluconolactone/gluconic acid in the exoskeleton. The remained body was also
107 subdivided in the 0.1N sodium acetate buffer (pH 4.0), and mashed by BioMasher II
108 (Nippi Inc, Tokyo, Japan) to extract metal ions and gluconic acid/gluconolactone. A
109 small amount of solution, which leaked from amphipod in the process of removing
110 exoskeletons, was also added. After centrifugation (5,000 x g, 10 min, 4°C), the
111 supernatant was divided into two layers of oil and water. Each layer was collected
112 separately. Then, precipitate was suspended in the same buffer and mashed again. After

113 centrifugation (5,000 x g, 10 min, 4°C), each oil and water layer was collected
114 separately. We gathered each layer to the first extraction, and used for measurements.

115 **Measurement of aluminum, iron, and gluconic acid/gluconolactone**
116 **content**

117 The aluminum content of the amphipod extract and water were measured using a
118 fluorometric analysis with 8-quinolinol [19]. We suspended samples in DDW, added
119 0.2 ml of 1% (wt./vol.) 8-quinolonol (Nacalai Tesque, Kyoto, Japan) and 0.2 ml of 2 N
120 CH_3COONa, and then added DDW to a volume of 5 ml. After mixing well, the
121 aluminum 8-quinolinol complex was extracted with 1 ml of chloroform. The aluminum
122 content was measured by the fluorescent intensity (excitation: 360 nm, emission: 535
123 nm). An aluminum chloride solution (Wako Pure Chemical Industries, Ltd.) was used
124 as the reference. The iron content of the extracted sediment or soil was measured at an
125 absorbance of 510 nm using Pack Test Fe (Kyouritu Chemical-Check Lab. Co., Tokyo,
126 Japan) based on the reaction of the Fe^{2+} ion and *o*-phenanthroline after reduction. An
127 iron (II) chloride solution was used as a reference. The D-gluconic acid/gluconolactone
128 content of the amphipods was measured using an E-kit "gluconic

129 acid/D-glucono-∂-lactone" (R-Biopharm AG, Damstadt, Germany). Sodium gluconic
130 acid (Wako Pure Chemical Industries, Ltd.) was used as a reference. We calculated total
131 amount of aluminum or gluconic acid/gluconolactone in amphipod from each measured
132 contents and volume of amphipod extracts.

133 **Effect of enzymatic degradation of gluconolactone/gluconic acid in the**
134 **extraction of *H. gigas* on the aluminum extraction ability**

135 We crushed and mashed a *H. gigas* individual with BioMasher II (Nippi Inc., Tokyo,
136 Japan). The mashed samples were centrifuged (3,000 x g, 10 min 4°C), and the body
137 fluid sample was collected. The precipitations were washed with 0.2 ml of DDW, and
138 then supernatant was collected and gathered with the body fluid sample after
139 centrifugation (3,000 x g, 10 min 4°C). The gathered sample was filtrated to remove
140 protein using a 3K Amicon Ultra 0.5 ml filter (Merck, Darmstadt, Germany). The pH
141 and volume of filtrated sample was adjusted to 8.0 with 0.1 N NaOH and 0.5 ml,
142 respectively. The 0.1 ml of samples and the same volume of enzyme reaction solution
143 of 0.2 M Tris-HCl buffer containing 20 mM ATP and 5.0 mM NADP were mixed, and
144 then added 1 U of gluconate kinase and 10 U of 6-phosphogluconate hydrogenase

(R-Biopharm AG, Darmstadt, Germany). The enzyme reaction was carried out at 25°C for 20 min. The reaction was stopped by filtration with 3K Amicon Ultra 0.5 ml filter. The pH of filtrate was adjusted to around 5.0 by the addition of HCl. The control reaction was also carried out without enzymes. The 0.1 ml of samples were mixed with the sediment of the Mariana Trench (0.1 g-dry weight) in 0.1 M sodium acetate buffer (pH 5.0). We incubated the mixture for 2 h at 4°C, 100 MPa. After centrifugation of mixture (5,000 x g, 10 min, 4°C), the aluminum content of the supernatant was measured.

High-pressure experiment with salmon roe

The salmon roe were purchased from a fish market. We washed the salmon roe with ice-cold artificial seawater (IWAKI CO., LTD, Tokyo, Japan) 3 times and then soaked them in the ice-cold artificial seawater. We created 16 tubes that each contained 4 salmon roe and artificial seawater, and we then added $AlCl_3$ (final conc.: 10 mM) to half of the tubes and adjusted the pH to 8.0 with 5 M NaOH. The tubes were then pressurized at 100 MPa or 0.1 MPa and incubated at 2°C for 1 day. After decompression, we observed the salmon roe and measured the protein concentration of

the artificial seawater using the Bradford method [20].

Cloning of cytochrome oxidase gene from the coastal amphipods

We extracted DNA from 10-20 coastal amphipods using DNAiso (Takara Bio Inc., Kyoto, Japan). The cytochrome oxidase I (COI) gene was amplified from the extracted DNA solution by PCR using the universal primer pair LCO1490 (5'-GGTCAACAAATCATAAAGATATTGG-3') and HCO2198 (5'-TAAACTTCAGGGTGACCAAAAAATCA-3') [21]. PCR amplification with a 50-µl reaction volume was performed using the GeneAmp PCR System 9700 (Applied Biosystems, Carlsbad, CA, USA) with EmeraldAmp (Takara Bio Inc., Otsu, Japan) and the buffer supplied with the enzyme. The PCR conditions were as follows: an initial incubation at 96°C for 30 s, 25 cycles of 98°C for 30 s, an incubation at 55°C for 30 s, another incubation at 72°C for 1 min, and a final extension at 72°C for 5 min. The PCR products were cloned in pT7blue-2 vector (Merck Millipore, MA, USA) and then transformed into *Escherichia coli* DH5a for blue/white selection. The cloned COI gene was amplified from the white colony by PCR using the same primers and conditions. The PCR products were analyzed by electrophoresis on a 1% agarose gel. The gel was

177 purified using Exo-SAP digestion with Exonuclease I (USB Corp., Cleveland, OH,
178 USA) and shrimp alkaline phosphatase (SAP) (Promega, Fitchburg, WI, USA) at 37°C
179 for 20 min and then treated at 80°C for 30 min to inactivate the enzymes. The PCR
180 products were sequenced using the primers described above and DYEnamic ET Dye
181 Terminator reagent (GE Healthcare Life Sciences, Piscataway, NJ, USA) on a
182 MegaBACE 1000 (Amersham Biosciences, Piscataway, NJ, USA) automatic sequencer.
183 The nucleotide sequences were trimmed, assembled, and translated using Sequencher
184 3.7 software (Gene Codes Corp., Ann Arbor, MI, USA).

185 **Phylogenetic analysis of the coastal amphipod**

186 A preliminary phylogenetic affiliation for each sequence was determined by conducting
187 a BLAST search. The most closely related sequences with representative
188 Lysianassoidean species sequences and certain outgroup sequences were aligned with
189 our sequences using CLUSTALX, and ambiguous regions were excluded from the
190 alignment. Phylogenetic trees were calculated with the PAML algorithm implemented
191 in the TOPALi package ver. 2.5 [22]. The statistical robustness of the analysis was
192 estimated by bootstrapping with 250 replicates.

Metabolome analysis of *H. gigas*

A metabolome analysis was conducted from 1 frozen *H. gigas* individual using capillary electrophoresis time-of-flight mass spectrometry (CE-TOFMS) and liquid chromatograph time-of-flight mass spectrometry (LC-TOFMS). The metabolome measurements were conducted through the services of a facility at the Human Metabolome Technology Inc., Tsuruoka, Japan.

CE-TOFMS

Approximately 45 mg of a frozen individual was plunged into 1.5 ml of 50% acetonitrile/Milli-Q water containing internal standards (H3304-1002, Human Metabolome Technologies, Inc., Tsuruoka, Japan) at 0°C to inactivate the enzymes. The individual was homogenized three times at 1,500 rpm for 120 s using a tissue homogenizer (Shake Master neo, Bio Medical Science, Tokyo, Japan), and then the homogenate was centrifuged at 2,300 × *g* at 4°C for 5 min. Subsequently, 800 µL of the upper aqueous layer was centrifugally filtered through a Millipore 5 kDa cutoff filter at 9,100 × *g* at 4°C for 120 min to remove proteins. The filtrate was centrifugally concentrated and re-suspended in 50 µl of Milli-Q water for the CE-MS analysis.

A CE-TOFMS analysis was conducted using an Agilent CE Capillary Electrophoresis System equipped with an Agilent 6210 TOF mass spectrometer, Agilent 1100 Isocratic HPLC pump, Agilent G1603A CE-MS adapter kit, and Agilent G1607A CE-ESI-MS sprayer kit (Agilent Technologies, Waldbronn, Germany). The systems were controlled by the software Agilent G2201AA ChemStation version B.03.01 for CE (Agilent

Technologies). The metabolites were analyzed using a fused-silica capillary (50 µm *i.d.* × 80 cm total length) and a commercial electrophoresis buffer (Solution ID: H3301-1001 for the cation analysis and H3302-1021 for the anion analysis, Human Metabolome Technologies) as the electrolyte. The sample was injected at a pressure of 50 mbar for 10 sec (approximately 10 nl) for the cation analysis and 25 sec (approximately 25 nl) for the anion analysis. The spectrometer was scanned from *m/z* 50 to 1,000. Other conditions were applied as previously described [23-25].

The automatic integration software MasterHands (Keio University, Tsuruoka, Japan) was used to obtain peak information, including the *m/z*, migration time for the CE-TOFMS measurement (MT) and the peak area [26]. Signal peaks corresponding to isotopomers, adduct ions, and other product ions of known metabolites were excluded, and the remaining peaks were annotated with putative metabolites from the HMT metabolite database based on their MTs and *m/z* values as determined by the TOFMS analysis. The tolerance range for the peak annotation was configured at ±0.5 min for MT and ±10 ppm for *m/z*. In addition, the peak areas were normalized against those of the internal standards, and the resultant relative area values were further normalized by the sample amount.

A hierarchical cluster analysis (HCA) and principal component analysis (PCA) were performed using our proprietary software PeakStat and SampleStat, respectively. The detected metabolites were plotted on metabolic pathway maps using VANTED (Visualization and Analysis of Networks containing Experimental Data) software [27].

LC-TOFMS

Approximately 45 mg of a frozen specimen was plunged into 0.5 ml of acetonitrile containing 1% formic acid and internal standards (H3304-1002, Human Metabolome

Technologies, Inc., Tsuruoka, Japan) at 0°C to inactivate the enzymes. The specimen was homogenized three times at 1,500 rpm for 120 s using a tissue homogenizer (Shake Master neo), and then 167 µl of Milli-Q water was added and homogenized once at 1,500 rpm for 120 s. The homogenate was centrifuged at 5,000 × *g* at 4°C for 5 min. The supernatant was used as a sample for the LC-TOFMS analysis, and a precipitate was homogenized once with 0.667 ml in the same solution at 1,500 rpm for 120 s. The homogenate of the precipitate was centrifuged at 5,000 × *g* at 4°C for 5 min. Both supernatants were mixed and centrifugally filtered through a Nanosep 3K (PALL Co., NY, US) at 9,100 × *g* at 4°C for 120 min to remove proteins. Solid phase extraction was conducted on the filtrate to remove phospholipids. The filtrate was centrifugally concentrated and re-suspended in 100 µl of 50% (v/v) isopropanol solution for the LC-TOFMS analysis.

The LC-TOFMS analysis was conducted using an Agilent 1200 series RRLC system SL (Agilent Technologies, CA, USA) and an ODS column (2×50 mm, 2 µm) equipped with an Agilent LC/MSD TOF system (Agilent Technologies). The LC analysis was performed using a mobile phase of solution A (H_2O/0.1%HCOOH) and solution B (isopropanol: acetonitrile: H_2O (65: 30: 5)/0.1% HCOOH, 2 mM $HCOONH_4$) at a gradient of 0-0.5 min: B 1%, 0.5-13.5 min: B 1-100%, 13.5-20 min: B 100%. Negative and positive modes were performed for the cationic and anionic metabolites. The MS system, measurement conditions, and analyses were conducted using the same procedures as described above for the CE-TOFMS analysis.

Result

Scanning electron microscopy (SEM)/energy dispersive X-ray spectrometry (EDS) analysis of *H. gigas* exoskeleton

First, we analyzed the elements of the exoskeletons of *H. gigas* captured from the Challenger Deep in the Mariana Trench using SEM/EDS. Our results showed a peak of aluminum as well as other major metals, such as calcium, magnesium, potassium, and sodium, in various parts of the exoskeleton (Fig. 1, Table 1). Calcium was most abundant in metal ions. Aluminum was widely distributed throughout the entire body, and an especially high content of aluminum was observed in the tail (telson) and along the edge the feet (pereopods, or uropods) (Fig. 1b-e, Supplementary Fig. 1). However, silicon, which is the major component of the clay mineral aluminosilicate [28, 29], was not observed; therefore, the aluminum in the exoskeleton was not derived from the aluminosilicate itself in sediment. We repeated the same analysis with other *H. gigas* individuals and obtained similar results, including a high aluminum content in their telson (S1, 2 Fig.). Similar to the amphipods from the Mariana Trench, the *H. gigas* specimens captured from the Izu-Ogasawara Trench also had aluminum in their exoskeleton (S3 Fig.). To identify whether the aluminum accumulated into exoskeleton

277 or adhered to surface of exoskeleton, we observed aluminum existence after washing
278 the surface of *H. gigas* individuals with distilled deionized water (DDW). The
279 aluminum was clearly removed from exoskeletons (Fig. 2). Therefore, the aluminum
280 covered the surface of exoskeleton rather then accumulation in the internal part of
281 exoskeleton. A comparison was performed to investigate the aluminum in the
282 exoskeleton of a shallow-sea, coastal amphipod that was captured from Maizuru Bay in
283 Japan and identified as *Prontogenesia* sp. based on the amino acid sequence of
284 cytochrome oxidase (S4 Fig.). Compared with the deep-sea amphipods, the SEM/EDS
285 analysis of the exoskeletons of *Prontogenesia* sp. did not show an aluminum peak (S5
286 Fig.). To date, aluminum content has not been reported in the exoskeletons of
287 crustaceans; however, we contend that exoskeletons containing aluminum is a unique
288 property of hadal amphipods.
289
290 **Figure 1. SEM/EDS analysis of the exoskeleton of *H. gigas*.**
291 *H. gigas* specimens captured from the Challenger Deep were freeze-dried for the SEM
292 observations. The SEM observations were conducted without any coating. Calcium

293 (red) and aluminum (green) were mapped on the SEM pictures (A, a-i). The EDS
294 spectrum included an annotation of each element with its Kα energy levels (C: 0.284,
295 O: 0.532, Na: 1.071, Mg: 1.253, Al: 1.486, P: 2.013, S: 2.307, Cl: 2.621, Ca: 3.69 (k
296 eV)).
297
298 **Figure 2 SEM/EDS analysis of the exoskeleton of *H. gigas* after washing with**
299 **DDW.**
300 Three *H. gigas* specimens captured from the Challenger Deep were washed 3 times with
301 DDW, and freeze-dried the SEM observations. The SEM observations were conducted
302 without any coating. Exoskeleton parts of the head (A, E, I), the body (B, F, J), the back
303 (C, G, K), and the telson (D, H, L) were observed. Each panel showed SEM image
304 (top), EDS spectrum (middle), and element composition obtained from EDS spectrum
305 (bottom).
306
307 Table 1. The ratio of atoms was calculated from the total spectrum count* in each panel
308 in Fig. 1

Atomic	Panel in Fig. 1							
(%)	a	b	c	d	e	f	g	h
C	69.43	53.82	67.33	55.32	63.91	67.06	57.20	55.46
N	0.00	0.00	0.00	0.00	0.00	0.00	2.29	0.00
O	25.11	34.78	21.65	34.95	24.26	28.85	35.41	38.25
Na	0.40	0.58	0.53	0.57	0.50	0.66	0.81	0.82
Mg	0.17	0.58	0.34	0.73	0.44	0.18	0.33	0.36
Al	0.07	3.33	1.27	0.53	3.10	0.03	0.03	0.05
P	0.39	0.64	0.82	0.19	0.13	0.32	0.38	0.51
S	0.00	0.00	0.00	1.60	0.00	0.11	0.16	0.12
Cl	0.33	0.41	0.72	0.57	0.61	0.33	0.40	0.41
K	0.06	0.00	0.07	0.10	0.00	0.02	0.03	0.04
Ca	4.04	5.86	7.25	5.45	6.11	2.44	2.96	3.99

*) The total spectrum counts were as follows: panel a: 321,710; panel b: 235,772; panel c: 235,233; panel d: 319,672; panel e: 171,886; panel f: 585,772; panel g: 540,040; and panel h: 400,863.

312

313 **Scanning transmission electron microscopy (STEM)/ EDS analysis of**

314 ***H. gigas* exoskeleton**

315 . We also observed the crushed exoskeleton to find aluminum of the internal

316 exoskeletons of *H. gigas* captured from the Challenger Deep through a scanning

317 transmission electron microscopy (STEM)/EDS analysis (Fig. 3). We found calcium in

318 all crushed exoskeleton, and nickel or copper in a few piece of exoskeleton. Copper and

319 nickel are minor elements in the marine sediment, and *H. gigas* would not accumulate

320 sufficient amounts for detection in the SEM/EDS analysis. The aluminum was not

321 contained in the internal exoskeleton. Silicate and molybdenum were background

322 signals from sample holder. We also observed the internal exoskeletons of the

323 amphipods captured from the Izu-Ogasawara Trench, and did not found any aluminum

324 peak in STEM/EDS analysis (S6 Figure).

325

326 **Figure 3 STEM/EDS analysis of pieces of *H. gigas* exoskeleton.**

327 Exoskeletons of *H. gigas* captured from the Challenger Deep were removed from the

328 individuals, freeze dried, and then scrapped. Bright-field STEM observations were
329 conducted for pieces of the exoskeletons (A, C, E, G). Characteristic X-rays were
330 collected over 60 s (B, D, F, H), and the major metal signals of panel E and G were
331 mapped (I, J). The Cu or Mo signals were caused by the TEM grid. The Si signal was
332 background.
333
334 **X-ray powder diffraction (XRD) analysis of the exoskeletons of *H. gigas***
335 We found calcium was major metal in the exoskeletons of *H. gigas* through EDS
336 analysis. Generally, it is known that calcium occurs as calcium carbonate and calcium
337 phosphate in the crustacean [30-32], however, much lower peak of phosphorus
338 compared with that of calcium was detected in the exoskeletons of *H. gigas* whose
339 habitat is much deeper than CCD (Table 1). This result indicates the possibility of the
340 existence of calcium carbonate in the exoskeleton. Thus, we carried out XRD analysis
341 of the exoskeletons of 5 individuals in order to examine existence of calcium carbonate
342 (Fig. 4). The diffraction peak positions in 5 samples were the same except for one
343 unknown peak. The 2θ of 7 main peaks was 23.1±0.1, 29.5, 36.0, 39.5, 43.2, 47.7, and

344 48.6, respectively. Since the crystal material in the exoskeleton was suggested to be
345 trigonal calcium carbonate from database search, calcium detected by the EDS analyses
346 was found to be mainly calcium carbonate. Compared with reference peak of crystal
347 calcium carbonate (CCC), the heights of peaks were decreased in accordance with the
348 increase of 2θ. Because CCC in the exoskeleton was made from amorphous calcium
349 carbonate (ACC), which was synthesized on chitin in crustacean [33-35], the observed
350 peaks are originated from both CCC and ACC. One unknown peak (2θ = 44.6) was
351 found in one sample, and suggested as AlO(OH) (1 1 1) (panel d). However, since we
352 could not find largest peak of AlO(OH) (1 1 0) (2θ = 22.3), we did not conclude that
353 this peak was originated from AlO(OH).
354

355 **Figure 4 XRD analysis of *H. gigas* exoskeleton**

356 Exoskeleton samples prepared from 5 individuals of *H. gigas* were used for XRD
357 analysis as described in Method (panel A-E). The annotations of peaks were results of
358 database search (panel F). Arrow in panel d indicates unknown peak, which was
359 suggested as AlO(OH) from library search. We cannot identified it as AlO(OH),

because other minor peaks were not found.

Aluminum content in *H. gigas*

Next, we measured the content of aluminum in the *H. gigas* individuals. To avoid the influence of aluminum oxide originating from the sediment, we used the 8-quinolinol method and applied the fluorescent label of the 8-quinolinol-aluminum ion complex [19]. We selected three individuals captured from the Challenger Deep in the Mariana Trench (S7 Fig.). The *H. gigas* exoskeletons of the three individuals contained over 50% aluminum and exhibited only minor differences in content (S1 Table), whereas the body fluid presented varying aluminum content among the 3 individuals. Because the crustaceans inhabiting contaminated areas accumulate metals in their gut [36, 37], the presence of aluminum in the exoskeleton indicated not to be a result of simple accumulation.

Identification of aluminum extraction agent *H. gigas*

Because aluminum is the third-most abundant element on Earth, possible origins of the aluminum in *H. gigas* include the marine sediment or the seawater. A large amount of aluminum occurs as aluminum oxide in the clay minerals of the marine sediment [28,

376 29, 38]. However, aluminum ions have been found in deep-sea water in small amounts
377 (approximately 2 nM) in the North Pacific [39, 40]. When deep-sea amphipods were
378 caught in the baited traps, the content in the digestive organ was the used bait, the
379 sediment, or nothing [5, 6]. We expected that *H. gigas* extracted aluminum from
380 sediment. In fact, an SEM/EDS analysis of another *H. gigas* individual showed the
381 presence of aluminum and silica in the head part, and element mapping showed the
382 same distribution of aluminum and silicon in the head (S8 Fig.). The atomic percent
383 calculated from each peaks were C: 49.2, N: 14.1, O: 30.5, Na: 0.42, Mg: 0.25, Al: 0.47,
384 Si: 1.66, P: 0.22, Cl: 0.32, Ca: 5.1, respectively. The ratio of aluminum and silicon was
385 approximately 1:3.53, which was similar to the aluminum ratio in the sediment
386 (1:3.34-1:4.96) (S2 Table) [41]. Accordingly, the aluminum found in *H. gigas* is likely
387 dependent on the release of aluminum from the marine sediment under the acidic
388 conditions of the gut, whose pH was estimated around 5-6 from the digestive enzyme
389 activities [6, 7, 42]. However, only a limited amount of aluminum was released from the
390 sediment of the Challenger Deep under the same physical conditions as observed in the
391 *H. gigas* gut or habitat (2°C, 100 MPa, and pH 5.0-8.0) [6, 7]. To examine the

392 extraction agent of aluminum from the sediment, we performed aluminum extraction
393 using the protein and non-protein fractions of crushed *H. gigas*, which are the enzymatic
394 or chemical reactions related to aluminum extraction, respectively. The results showed
395 that the non-protein fraction could extract aluminum (Fig. 5); therefore, we conducted a
396 metabolome analysis of an entire *H. gigas* individual to identify the chemicals that
397 contribute to releasing aluminum from the sediment. The results indicated that *H. gigas*
398 produces 217 chemicals (S3 Table). As potential candidates, we focused on 60
399 chemicals that are not involved in the metabolic pathways of the animal because
400 metabolites involved in these pathways usually occur in the inner cells and cannot react
401 to extracellular marine sediment in the gut. Among the 60 chemicals, gluconic
402 acid/gluconolactone (gluconolactone in acidic pH) is known as a strong organic
403 chelating agent [43]. A high glucose content (0.43%±0.1% (w/w) (dry weight)) was
404 present in the *H. gigas* individuals, which is a source of gluconic acid/gluconolactone
405 [6]. Furthermore, gluconic acid/gluconolactone levels of 0.3-0.4 mM were measured in
406 the bodies of the *H. gigas* presented here (S4 Table). We examined the effects of
407 gluconic acid/gluconolactone on the release of aluminum from the sediment of the

408 Challenger Deep and confirmed that gluconic acid/gluconolactone released the
409 aluminum ion from the sediment at pH 6.2 or lower under *in situ* conditions (Fig. 6).
410 Under acidic conditions, gluconolactone is a main component in the chemical equation
411 of gluconic acid/gluconolactone and acts as an extraction agent of aluminum from
412 sediment in the gut [43]. Therefore, the extraction of aluminum is a unique property of
413 gluconolactone, rather than a chelating activity of gluconic acid. When we removed
414 gluconic acid/gluconolactone from the extraction of *H. gigas* with enzymatic reaction of
415 gluconokinase (EC 2.7.1.12), the ability of aluminum extraction form sediments was
416 lost (S9 Fig.). Gluconolactone was main aluminum extractor in *H. gigas*. Gluconic
417 acid/gluconolactone can extract minor amounts of iron from sediment under the same
418 deep-sea bottom conditions (S10 Fig.). Therefore, copper and nickel, found in
419 STEM/EDS observation, were also included in and extracted from the sediment by
420 gluconic acid/gluconolactone [29, 43].

421

422 **Figure 5 Extraction of aluminum from the sediment of Challenger Deep by the *H.***
423 ***gigas* protein fraction or non-protein fraction.** Three *H. gigas* individuals were

424 scrapped and then suspended in 1 ml of $(NH_4)_2SO_4$ solution at 80% saturation. After
425 incubation at 4°C for 2 h, the *H. gigas* suspensions were centrifuged at 20,000 x *g* for
426 30 min. The supernatants were used as the non-protein fractions, and the precipitates
427 were suspended in 1 ml of DDW to prepare the protein fractions. We mixed 300 µl of
428 each fraction with the sediment suspension and added sodium acetate buffer to a final
429 volume of 1.8 ml (final concentration: 50 mM, pH 5.0). The mixtures were then
430 pressurized at 100 MPa and incubated at 2°C. After 1 h incubation, the mixtures were
431 de-pressurized and centrifuged at 20,000 x *g* for 10 min. The aluminum content of the
432 supernatants was measured as described in the Methods section. The error bar shows the
433 S.D. (n=3).
434
435 **Figure 6 Extraction of aluminum from the sediment of Challenger Deep by**
436 **gluconic acid/gluconolactone.**
437 Sediment samples were washed with distilled deionized water five times and then
438 suspended in each buffer, which contained 10 mM sodium gluconic acid/gluconolactone
439 (closed circle) or not (open circle). Extracted aluminum was measured as described in

440 the Materials and Methods.

441

442 # Discussion

443 We have shown that aluminum hydroxide gel covers the body of *H. gigas* in this study.

444 *H. gigas* inhabits the bottom of the deepest trench by obtaining glucose, a resource of

445 gluconolactone/gluconic acid, from plant debris buried in sediment digested by their

446 own cellulase and hemicellulose hydrolases [5-7]. Namely, *H. gigas* has ability to take

447 in both resources of aluminum and it's extraction agent from the sediment. Aluminum

448 hydroxide gel is constructed by chemical behavior of aluminum ion toward pH. The

449 extracted aluminum ions in the gut are released to the seawater of around pH 8, where

450 they are transformed to the gel state of aluminum hydroxide and then mainly stored in

451 the *H. gigas* telson [44, 45]. The aluminum spread on the surface of exoskeleton

452 without discharging together with excrement. Thus, it is thought that *H. gigas* has some

453 transport system of aluminum. We also detected gluconic acid in the exoskeletons at

454 0.06-0.16 μmol per individual (S4 Table), which turns into gluconic acid from

455 gluconolactone in contact with the alkaline seawater.as excrement. Hence, there would

456 be some transporter of aluminum in *H. gigas*. The converted gluconic acid would work
457 as a chelating agent for transferring aluminum ions to whole exoskeleton. The binding
458 property and stability of aluminum hydroxide gel to organisms are still unclear. The
459 aluminum hydroxide gel can be stable only in alkaline environment. Therefore,
460 "aluminum cover" would present only in the lives inhabiting the ocean and some
461 alkaline lakes.

462 Because the amphipods captured from the Izu-Ogasawara Trench were also found to
463 have the aluminum hydroxide gel, the aluminum hydroxide gel may have some
464 common role for the protection from the high pressure in the deep sea. Thus, we carried
465 out a preliminary experiment to figure out protection effect of aluminum hydroxide gel
466 on high pressure stress using salmon roes, and found less protein leak and no color
467 change in the presence of aluminum hydroxide gel even under 100 MPa (S11 Fig.). The
468 aluminum hydroxide gel may contribute to the adaptation system in the high pressure.
469 However, since the surface of salmon roe is very different from that of amphipod's
470 exoskeleton, we should do the same experiments using good analogous animal samples
471 of *H. gigas* although it is difficult to find them for better understanding of the properties

472 of aluminum in *H. gigas*.

473 Discovery of CCC in the exoskeleton of *H. gigas* indicated that CCD did not govern
474 synthesis of biological calcium carbonate. But in contrast to our discovery, the
475 foraminifera living under CCD don't have calcium carbonate shell [18, 46]. Thus, the
476 difference of structural or chemical composition between amphipod and foraminifera
477 would be related with the retention of calcium carbonate. In any case, the effect of
478 aluminum gel on synthesis and maintenance of crystal carbonate is still unknown.

479

480 Author Contributions

481 H. K. designed and performed all experiments and wrote the paper. H. K., H. S. and Y.
482 N. prepared the amphipod samples for electron microscopy observations and performed
483 the SEM/EDS and STEM/EDS analyses. H. K., W. A., and H. T. prepared the baited
484 traps and captured *H. gigas* from the Mariana Trench and the Izu-Ogasawara Trench.
485 All authors discussed the results and commented on the manuscript.

486

487 Material and Correspondance

488 All materials and correspondence should be addressed to Hideki Kobayashi

489

490 Competing financial interests

491 The authors declare no competing financial interests.

492

493 Data availability

494 Sequencing data of COI have been deposited in DDBJ with the accession codes
495 "LC085650-LC085655"
496 (http://getentry.ddbj.nig.ac.jp/getentry/na/LC085650-LC085655).

497

498 Reference

499 1. Wüst G. The major deep-sea expeditions and research vessels 1873-1960: a
500 contribution to the history of oceanography. Progress in Oceanography. 1964;2:
501 1-52.
502 2. Jamieson AJ, Fujii T, Mayor DJ, Solan M, Priede IG. Hadal trenches: the ecology
503 of the deepest places on Earth. Trends Ecol & Evol. 2010;25: 190-197.
504 3. Alan J. Chap. 9 Crustacea in Alan J editor. The hadal zone: life in the deepest
505 oceans. Cambridge Univ. Press; 2015. pp169-216.

506 4. Eustace RM, Kilgallen NM, Lacey NC, Jamieson AJ. Population structure of the
507 hadal amphipod Hirondellea gigas from the Izu-Bonin Trench (NW Pacific; 8173–
508 9316 m). J Crust Biol. 2013;33: 793–801.
509 5. Hessler RR, Ingram LC, Yayanos AA, Burnett RB. Scavenging amphipods from
510 floor of the Philippine Trench. Deep Sea Res. 1978;25: 1029-1047.
511 6. Kobayashi H, Hatada Y, Tsubouchi T, Nagahama T, Takami H. The hadal
512 amphipod *Hirondellea gigas* possessing a unique cellulase for digesting wooden
513 debris buried in the deepest seafloor. PLoS ONE 7. e42727. doi:10.1371. 2012.
514 7. Kobayashi H, Nagahama T, Arai W, Sasagawa Y, Umeda M, et al. Polysaccharide
515 hydrolase of the hadal zone amphipods *Hirondellea gigas*. Biosci Biotech
516 Biochem. 2018;82: 1123-1133.
517 8. Ritchiea H, Jamiesonb AJ, Piertney SB. Phylogenetic relationships among hadal
518 amphipods of the Superfamily *Lysianassoidea*: Implications for taxonomy and
519 biogeography. Deep Sea Res. 2015;I: 105, 119-131.
520 9. Pearcy WG, Ambler JW. Food habits of deep-sea macrourid fishes off the Oregon
521 coast. Deep Sea Res. 1974;21: 745-59.
522 10. McLellan T, Feeding strategies of the macrourids. Deep Sea Res. 1978;24:

523 1019-1036.

524 11. National Geographic, Watch. 2014 Dec.: World's Deepest Fish Lurks 5 Miles
525 Down in Mariana Trench. Available from:
526 http://news.nationalgeographic.com/news/2014/12/141219-deepest-fish-mariana-tr
527 ench-animal-ocean-science/.

528 12. Thiede J, Agdestein T. Strand JE. Depth distribution of calcareous sediments in the
529 Mesozoic and Cenozoic North Atlantic Ocean. Earth and Planetary Science Letters
530 1980;47: 416-422.

531 13. Whatley RC, The bonds unloosed: the contribution of Ostracoda to our
532 understanding of deep-sea events and processes. in Moguilevsky A, Whatley RC
533 editors. Microfossils and Oceanic Environments. University of Wales,
534 Aberystwyth Press;1996. pp3-25.

535 14. Boomer I. Late Cretaceous and Cainozoic bathyal Ostracoda from the Central
536 Pacific (DSDP Site 463). Marine Micropaleontology. 1999;37: 131–147.

537 15. Coles GP, Whatley RC, Moguilevsky A. The ostracod genus *Krithe* from the
538 Tertiary and Quaternary of the North Atlantic. Palaeontology. 1994;37: 71–120.

539 16. Jellinek T, Swanson K, Mazzini I. Is the cosmopolitan model still valid for
540 deep-sea podocopid ostracods? With the discussion of two new species of the
541 genus Pseudobosquetina Guernet & Moullade 1994 and Cytheropteron testudo
542 (Ostracoda) as case studies. Senckenbergiana Maritima. 2006;36: 29–50.
543 17. Schmiedl G, Mackensen A, Muller PJ. Recent benthic foraminifera from the
544 eastern South Atlantic Ocean: dependence on food supply and water masses.
545 Marine Micropaleontology. 1997;32: 249–287.
546 18. Todo Y, Kitazato H, Hashimoto J, Gooday AJ. Simple foraminifera flourish at the
547 ocean's deepest point. Science. 2005;307: 689.
548 19. Goon E, Petley JE, McMullen WH, Wiberley SE. Fluorometric determination of
549 aluminum:use of 8-quinolinol. Anal Chem. 1953;25: 608-610.
550 20. Bradford MM. A rapid and sensitive method for the quantitation of microgram
551 quantities of protein utilizing the principle of protein- dye binding. Anal Biochem.
552 1976;72: 248–254.
553 21. Folmer O, Black M, Hoeh W, Lutz R, Vrijenhoek R. DNA primers for
554 amplification of mitochondrial cytochrome c oxidase subunit I from diverse

555 metazoan invertebrates. Mol Mar Biol Biotechnol. 1994;3: 294-299.

556 22. Milne I, Lindner D, Bayer M, Husmeier D, McGuire G, et al. TOPALi v2: a rich
557 graphical interface for evolutionary analyses of multiple alignments on HPC
558 clusters and multi-core desktops. Bioinformatics. 2009;25: 126-127.

559 23. Soga T, Heiger DN. Amino acid analysis by capillary electrophoresis electrospray
560 ionization mass spectrometry. Anal.Chem. 2007;72: 1236–1241.

561 24. Soga T. Ueno Y, Naraoka H, Ohashi Y, Tomita M, et al. Simultaneous
562 determination of anionic intermediates for *Bacillus subtilis* metabolic pathways by
563 capillary electrophoresis electrospray ionization mass spectrometry. Anal Chem.
564 74;2002: 2233–2239.

565 25. Soga T. Ohashi Y, Ueno Y, Naraoka H, Tomita M, et al. Quantitative metabolome
566 analysis using capillary electrophoresis mass spectrometry. J Proteome Res.
567 2003;2: 488–494.

568 26. Sugimoto M, Wong DT, Hirayama A, Soga T, Tomita M. Capillary electrophoresis
569 mass spectrometry-based saliva metabolomics identified oral, breast and pancreatic
570 cancer–specific profiles. Metabolomics. 2009;6: 78–95.

571 27. Junker BH, Klukas C, Schreiber F. VANTED: A system for advanced data
572 analysis and visualization in the context of biological networks. BMC

573 Bioinformatics. 2006;7: 109.

574 28. Taylor SR. Abundance of chemical elements in the continental crust: a new table.
575 Geochim. cosmochim. Acta. 1964;28, 1273−1285.

576 29. Kato Y, Fujinaga K, Nakamura K, Takaya Y, Kitamura K, et al. Deep-sea mud in
577 the Pacific Ocean as a potential resource for rare-earth elements. Nat Geosci.
578 2011;4: 535–539.

579 30. Boßelmann F, Romano P, Fabritius H, Raabe D, Epple M. The composition of the
580 exoskeleton of two crustacea: The American lobster *Homarus americanus* and the
581 edible crab *Cancer pagurus*. Thermochimica Acta, 2007;463: 65-68.

582 31. Neues F, Ziegler A, Epple M. The composition of the mineralized cuticle in marine
583 and terrestrial isopods: a comparative study. Cryst Eng Comm, 2007;9: 1245-1251.

584 32. Becker A, Ziegler A, Epple M. The mineral phase in the cuticles of two species of
585 Crustacea consists of magnesium calcite, amorphous calcium carbonate and
586 amorphous calcium phosphate. Dalton Trans. 2005;10: 1814–1820.

587 33. Luquet G, Marin F. Biomineralisations in crustaceans: storage strategies. C R
588 Palevol, 2004;3: 515-534.

589 34. Pouget EM, Bomans PH, Goos JA, Frederik PM, Sommerdijk NA. The initial

stages of template-controlled CaCO3 formation revealed by cryo-TEM. Science. 2009;323: 1455-1458.

35. Sato A, Nagasaka S, Furihata K, Nagata S, Arai I, et al. Glycolytic intermediates induce amorphous calcium carbonate formation in crustaceans. Nat Chem Biol. 2011;7: 197-199.

36. Viarengo A. Heavy metals in marine invertebrates: mechanisms of regulation and toxicity at the cellular level. CRC Crit Rev Aquat Sci. 1989;1: 295–317.

37. Ahearn GA, Mandal PK, Mandal A. Mechanisms of heavy-metal sequestration and detoxification in crustaceans: a review. J. comp. Physiol. B 2004;174: 439-452.

38. Seibold E, Berger WH. The Sea Floor- An Introduction to Marine Geology. 3rd ed. Springer: 1996.

39. Orians KJ, Bruland KW. Dissolved aluminium in the central North Pacific, Nature 316;1985: 427-429.

40. Kramer J, Lean P, Sarthou G, Timmermans KR, de Baar HJW. Distribution of dissolved aluminium in the high atmospheric input region of the subtropical waters of the North Atlantic Ocean. Maine Chemistry. 2004;88: 85-101.

606 41. Goldberg ED, Arrhenius GOS. Chemistry of Pacific pelagic sediments. Geochim.
607 Cosmochim. Acta. 1958;13: 153-212.
608 42. Kombo MM, Vual SA, Ishiki M, Tokuyama A. Influemce of salinity on pH and
609 aluminum concentration on the interaction of acidic red soil with seawater. J
610 Oceanography. 2005;61: 591-601.
611 43. Mitchell RE, Duke FR. Kinetics and equilibrium constants of the gluconic
612 acid-gluconolactone system. Ann NY Acad Sci. 1970;172: 131-138.
613 44. Wefers K, Misra C. Oxides and Hydroxides of Aluminum; ALCOA, Laboratories,
614 Pennsilvania, USA. 1987: pp.1-10.
615 45. Armstrong J, Martin M. An in vitro evaluation of commonly used antacids with
616 special reference to aluminium hydroxide gel and dried aluminium hydroxide gel. J
617 Pharm Pharmacol, 1953;5: 672-685.
618 46. Sabbatini A, Morigi C, Negri A, Gooday AJ. Soft-shelled benthic foraminifera
619 from a hadal site (7800 m water depth) in the Atacama Trench (SE Pacific):
620 preliminary observations. J Micropalaeontol, 2002;21: 131-135.

621

622

623 Supporting information

S1 Figure SEM/EDS analysis of the exoskeleton of *H. gigas* telson.

H. gigas specimens captured from Challenger Deep was freeze dried for SEM observations (A, B). Panel B shows an enlargement of the red square in panel A. SEM observations and EDS analyses were conducted without any coating. The EDS spectrum of panel B includes an annotation of each element with its Kα energy level (C: 0.284, O: 0.532, Na: 1.071, Mg: 1.253, Al: 1.486, P: 2.013, S: 2.307, Cl: 2.621, Ca: 3.69 (k eV)) (C). The total spectrum counts were 117,388 in the EDS analysis, and the major elements were mapped (D).

S2 Figure SEM/EDS analysis of the *H. gigas* exoskeleton.

An SEM/EDS analysis was conducted on the telson region (A) and the exoskeleton (E) as described in the Methods section. The EDS spectra of panel A and E include annotations of each element with its Kα energy level (C: 0.284, O: 0.532, Na: 1.071, Mg: 1.253, Al: 1.486, P: 2.013, S: 2.307, Cl: 2.621, Ca: 3.69 (k eV)) (B, F). The metal peaks were mapped for the telson (C) and the exoskeleton (G). The composition of elements was calculated from the total spectrum counts (D: 320,357, H: 141,002).

S3 Figure SEM/EDS analysis of *H. gigas* captured from the Izu-Ogasawara

640 **Trench.**

641 An SEM/EDS analysis was conducted on *H. gigas* captured from the Izu-Ogasawara
642 Trench. Four views of the exoskeleton were analyzed (A, E, I, M) as described in the
643 Methods section. Panels E, I, and M were observed with accelerating voltages of 15 kV,
644 because oil components induce sample charging and cause drift in SEM/EDX images,
645 which cannot be suppressed at high acceleration voltage sufficiently. Only calcium and
646 aluminum were mapped (B, F, J, N). The EDS spectrum includes an annotation of each
647 element with its Kα energy level (C: 0.284, O: 0.532, Na: 1.071, Mg: 1.253, Al: 1.486,
648 P: 2.013, S: 2.307, Cl: 2.621, Ca: 3.69 (k eV)). All EDS signals were detected and
649 calculated from the total spectrum counts (C and D, G and H, K and L, O and P).

650 **S4 Figure Phylogenetic tree of the captured coastal amphipods and related**
651 **amphipods reconstructed from the mitochondrial COI protein sequence alignment**
652 **(192 amino acids).**

653 The COI genes were amplified and cloned in *E. coli* DH5α as described in the Methods
654 section. Then, we decided DNA sequences of 6 *E. coli* clones. The amino acid sequence
655 of the COI obtained from the coastal amphipods indicated “clone1-6” in this study. The

656 amino acid sequences of the COI of related amphipods were obtained from GenBank,
657 and each accession number was added after the species name. Bold lines indicate
658 bootstrap support above 95% as inferred from the maximum likelihood analysis. The
659 scale bar for the branch length is denoted by the estimated number of amino acid
660 substitutions per site.

661 **S5 Figure SEM/EDS analysis of the coastal amphipods.**

662 Three amphipods were freeze dried and then analyzed. The telson (A, C) and foot (E) of
663 *H. gigas* contained aluminum. Panel A and B were observed with accelerating voltages
664 of 10 kV because of sample movement related to the oil component. EDS analysis was
665 conducted as described in the Methods section (B, D, F). The EDS spectrum includes an
666 annotation of each element with its Kα energy level (C: 0.284, O: 0.532, Na: 1.071, Mg:
667 1.253, P: 2.013, S: 2.307, Cl: 2.621, Ca: 3.69 (k eV)). The peak of Si was obtained from
668 the backfield in F.

669 **S6 Figure STEM/EDS analysis of pieces of the deep-sea amphipod's exoskeleton.**

670 Exoskeletons of the amphipods captured from the Izu-Ogasawara Trench were removed
671 from the individuals, freeze dried, and then scrapped. Bright-field STEM observations

672 were conducted for pieces of the exoskeletons (A, C, E). Characteristic X-rays were
673 collected over 60 s (B, D, F). The Cu or Mo signals were caused by the TEM grid. The
674 Si signal was background.

675 **S7 Figure *H. gigas* individuals used for the aluminum measurements.**

676 Deep-sea amphipod *H. gigas* individuals were immediately frozen and maintained at
677 -80°C after capture from Challenger Deep. These amphipods were selected randomaly
678 from frozen stock.

679 **S8 Figure SEM/EDS analysis of the exoskeleton of the head of *H. gigas*.**

680 *H. gigas* specimens captured from Challenger Deep were freeze dried for the SEM
681 observations (A). SEM observations were conducted without any coating. The EDS
682 spectrum included an annotation of each element with its Kα energy level (C: 0.284, O:
683 0.532, Na: 1.071, Mg: 1.253, Al: 1.486, Si: 1.739, P: 2.013, S: 2.307, Cl: 2.621, Ca:
684 3.69 (k eV)) (B). The total spectrum counts were 141821 in the EDS analysis, and the
685 signals of Si, Al and Ca were mapped (C).

686 **S9 Figure Effect of gluconic acid/gluconolactone removal on aluminum extraction**
687 **capacity of *H. gigas* body fluid** Three *H. gigas* individuals were used for the

688 experiment. We prepared *H. gigas* body fluid and removed gluconic
689 acid/gluconolactone from *H. gigas* body fluid with enzymes as described in Materials
690 and Methods (enzyme treated sample. Control sample was prepared without enzyme
691 (control).

692 **S10 Figure Extraction of iron from the sediment of Challenger Deep.**

693 The sediment was suspended in 25 mM sodium acetate buffer (pH 5.0) containing 10
694 mM sodium gluconic acid/gluconolactone or not (control). The suspension was
695 pressurized at 100 MPa and incubated at 2°C for 1 h. After decompression, the sediment
696 was separated with centrifugation (15,000 x *g* at 4°C for 2 min). The iron content of the
697 supernatant was measured as described in the Methods section. The error bar shows the
698 S.D. (n=3).

699 **S11 Figure Effect of aluminum hydroxide gel on the release of protein from**
700 **salmon roe under high pressure.**

701 Washed salmon roe were soaked and pressurized in artificial seawater at 100 MPa,
702 which is the same pressure observed at approximately 10,000 m in depth, or in the
703 control at 0.1 MPa, which is the same pressure observed in the atmosphere at sea level,

704 for 24 h in a pressure-resistant bottle. The salmon roe that suffered the greatest damage

705 after decompression are displayed in panel A. After decompression, the protein content

706 of the artificial seawater was measured (panel B). The error bar shows the S.D. (n=4).

707 The bar in panel A indicates 1 cm.

708 **Supplementary Table 1 Amount of aluminum in the body of *H. gigas***

709 **Supplementary Table 2 The TEM/EDS analysis of the sediments**

710 **Supplementary Table 3 Metabolic analysis of *H. gigas***

711 **Supplementary Table 4 Amount of gluconic acid in the body of *H. gigas***

712

713

Figure 1 Kobayashi et al.

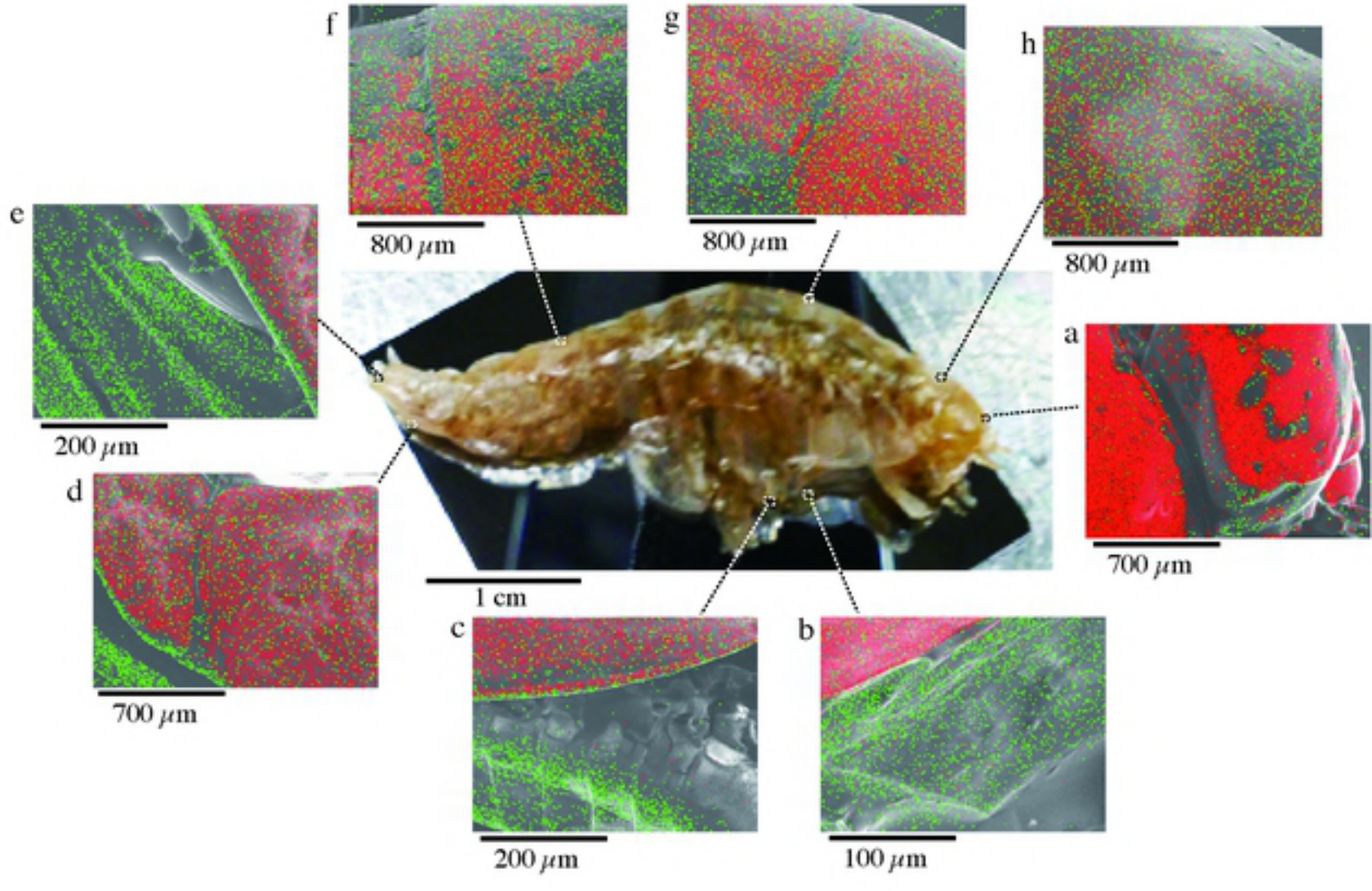

Fig.1

Individual No. 1

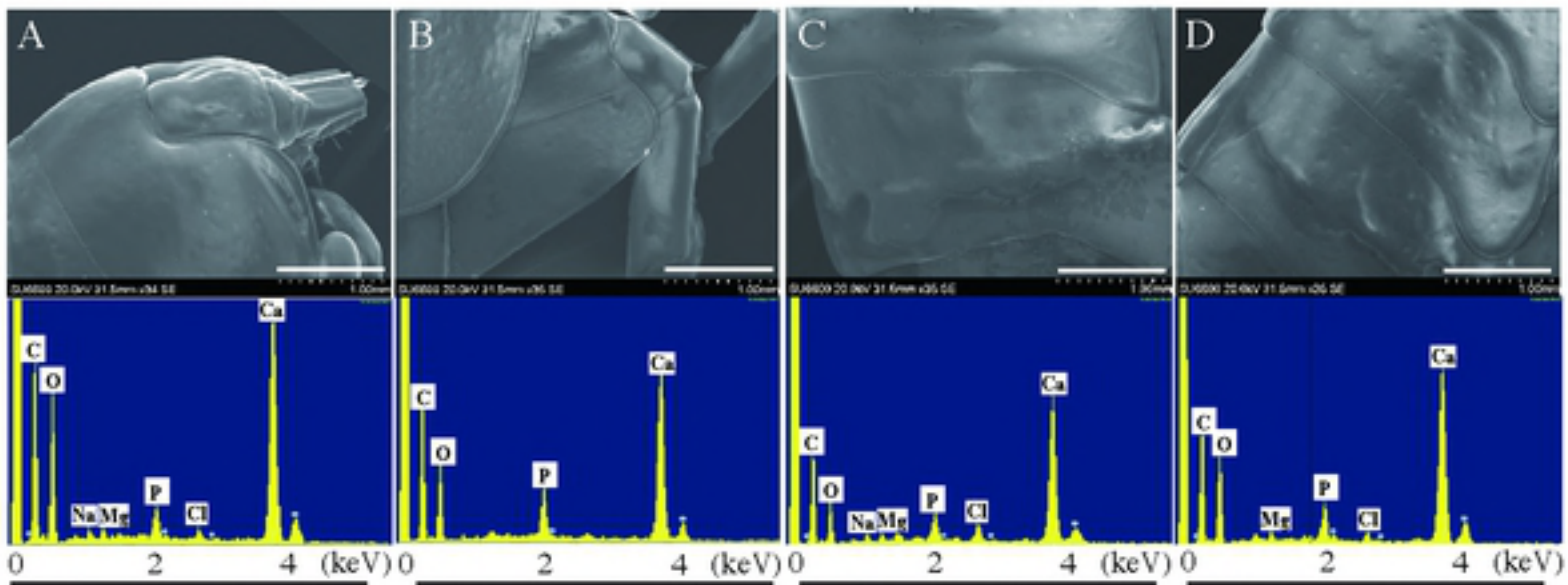

Elements	Atom (%)
C	47.80
O	43.86
Na	0.51
Mg	0.36
P	0.84
Cl	0.27
Ca	6.35

Elements	Atom (%)
C	52.68
O	38.42
Ca	8.91

Elements	Atom (%)
C	55.58
O	32.03
Na	0.81
Mg	0.57
P	1.40
Cl	0.84
Ca	8.75

Elements	Atom (%)
C	47.77
O	42.48
Na	0.46
P	1.45
Cl	0.29
Ca	7.55

Individual No. 2

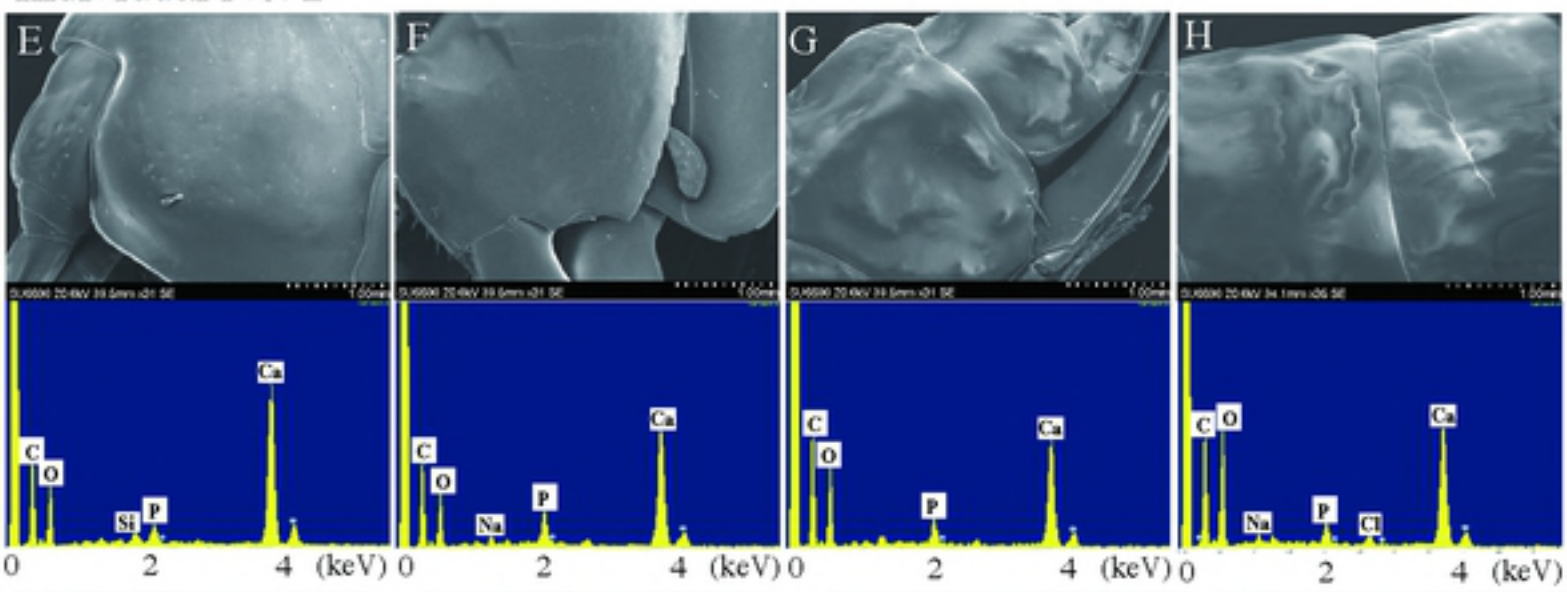

Elements	Atom (%)
C	44.88
O	43.68
Si	0.46
P	1.00
Ca	9.98

Elements	Atom (%)
C	50.38
O	39.33
Na	0.67
P	1.99
Ca	7.62

Elements	Atom (%)
C	50.16
O	42.90
P	1.25
Ca	5.68

Elements	Atom (%)
C	45.28
O	47.54
Na	0.75
P	0.90
Cl	0.36
Ca	5.17

Individual No. 3

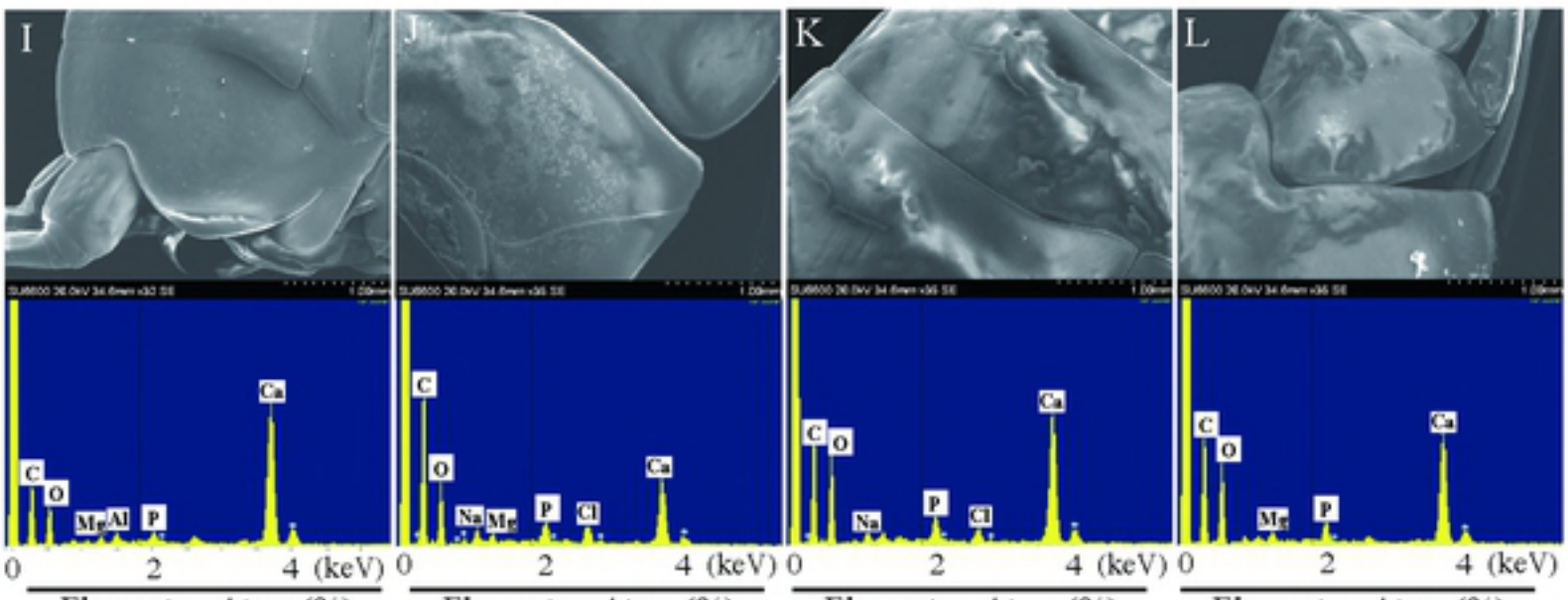

Elements	Atom (%)
C	43.72
O	42.39
Mg	0.76
Al	0.66
P	0.71
Ca	11.77

Elements	Atom (%)
C	64.48
O	29.84
Na	0.95
Mg	0.45
P	0.77
Cl	0.73
Ca	2.79

Elements	Atom (%)
C	48.40
O	43.20
Na	0.84
P	1.03
Cl	0.57
Ca	5.96

Elements	Atom (%)
C	48.57
O	43.74
Mg	0.59
P	1.05
Ca	6.06

Fig.2

Figure 3 Kobayashi etal.

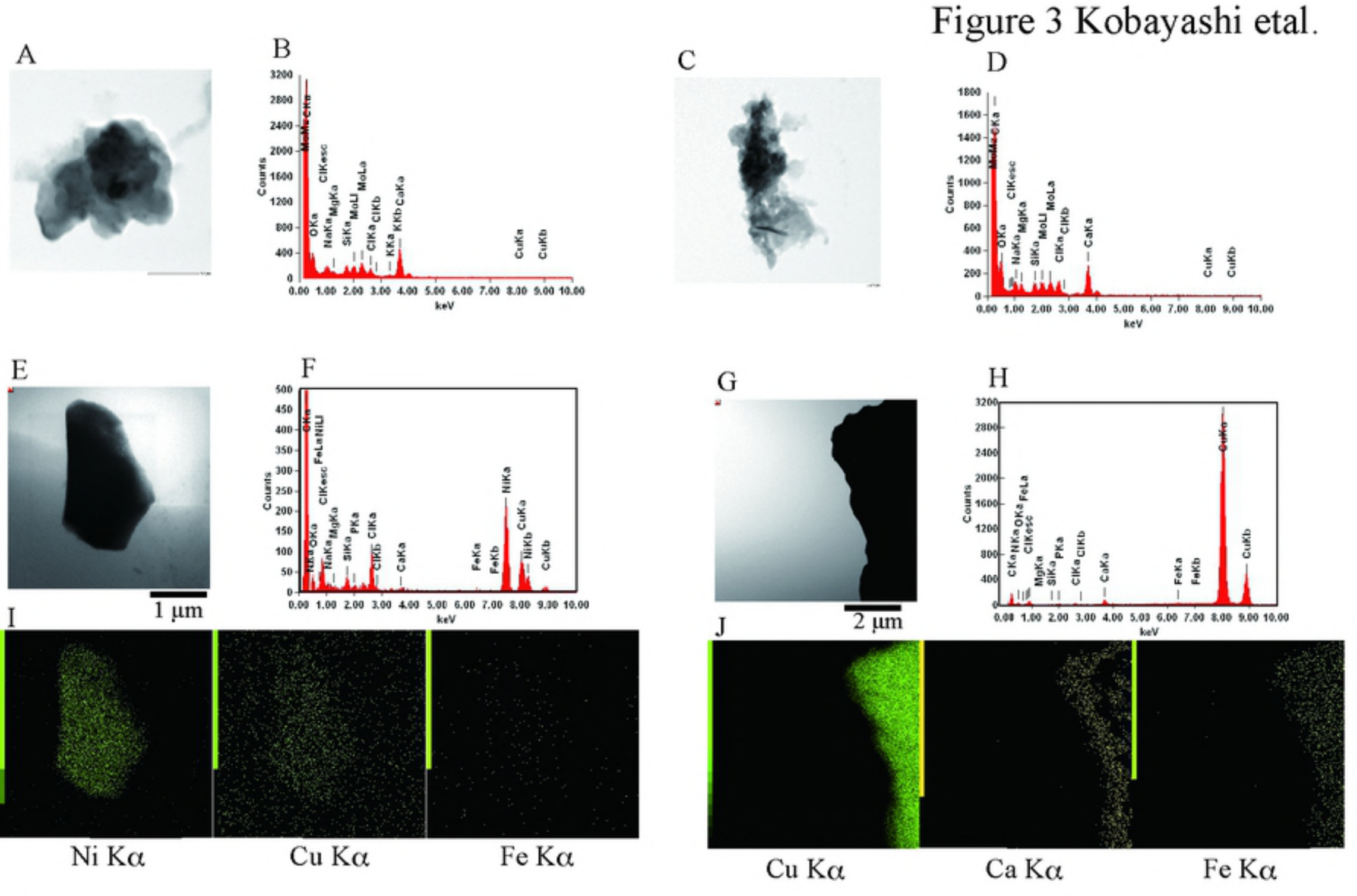

Fig.3

Figure 4 Kobayashi et al.

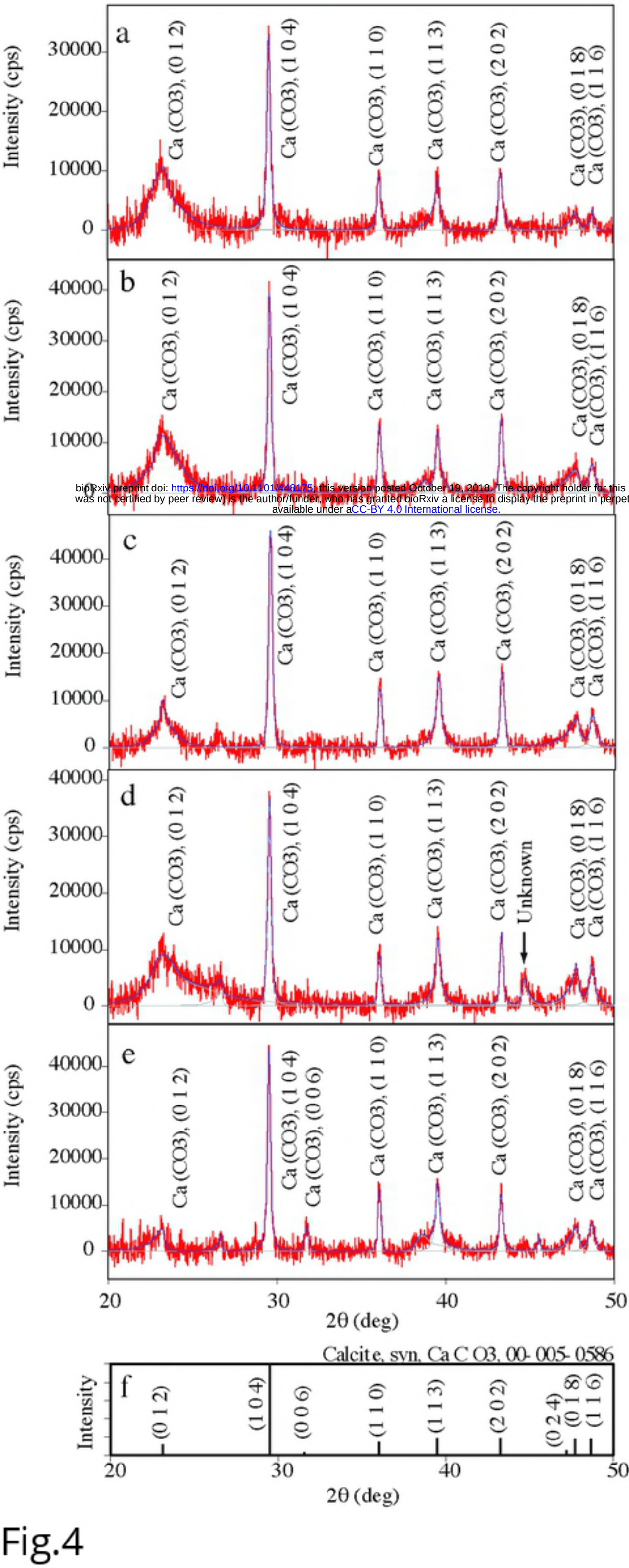

Fig.4

Figure 5 Kobayashi et al.

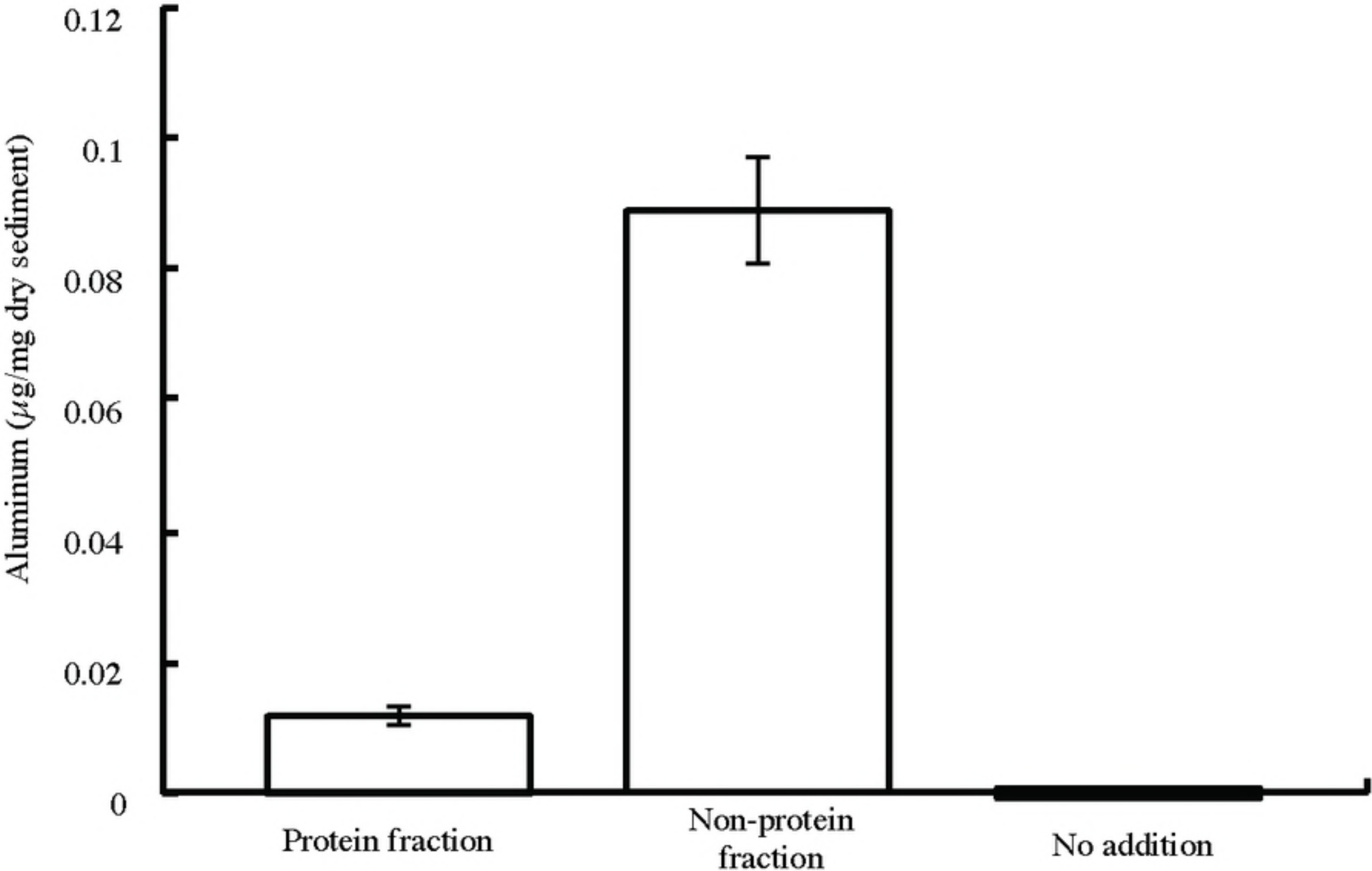

Fig.5

Figure 6 Kobayashi et al.

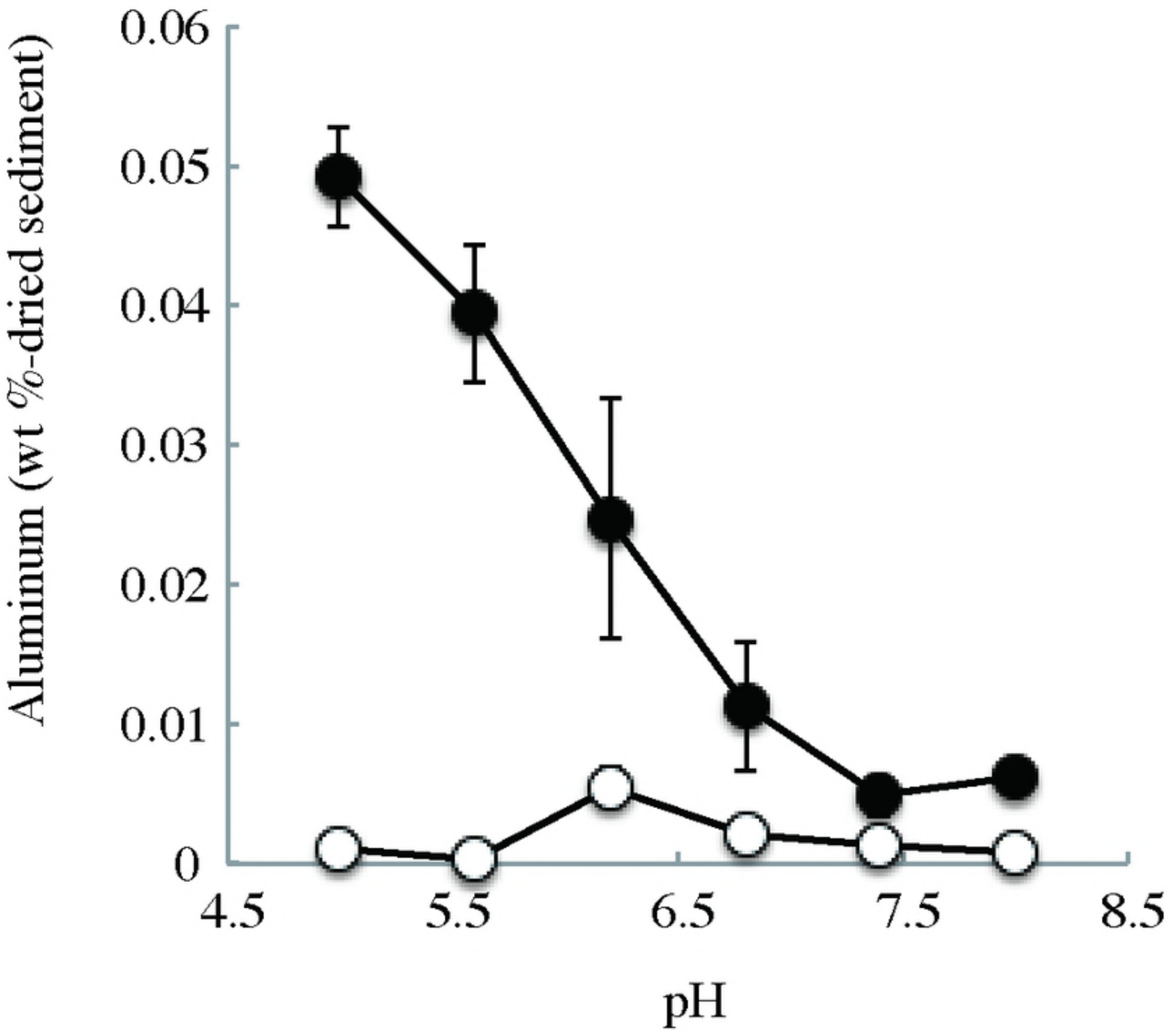

Fig.6